The Astrophysical Journal Letters, 816:L17 (4pp), 2016 January 1 doi:10.3847/2041-8205/816/1/L17
© 2016. The American Astronomical Society. All rights reserved.

# SURFACE TEMPERATURES ON TITAN DURING NORTHERN WINTER AND SPRING

D. E. Jennings[1], V. Cottini[1,2], C. A. Nixon[1], R. K. Achterberg[1,2], F. M. Flasar[1], V. G. Kunde[1], P. N. Romani[1], R. E. Samuelson[1,2], A. Mamoutkine[3], N. J. P. Gorius[4], A. Coustenis[5], and T. Tokano[6]

[1] Goddard Space Flight Center, Greenbelt, MD 20771, USA; donald.e.jennings@nasa.gov
[2] Department of Astronomy, University of Maryland, College Park, MD 20742, USA
[3] ADNET Systems, Inc., Bethesda, MD 20817, USA
[4] The Catholic University of America, Washington, DC 20064, USA
[5] Laboratoire d'Etudes Spatiales et d'Instrumentation en Astrophysique (LESIA), Observatoire de Paris, CNRS, UPMC Univ. Paris 06, Univ. Paris-Diderot, 5, place Jules Janssen, F-92195 Meudon Cedex, France
[6] Universität zu Köln, Albertus-Magnus-Platz, D-50923 Köln, Germany
*Received 2015 November 25; accepted 2015 December 15; published 2016 January 4*

## ABSTRACT

Meridional brightness temperatures were measured on the surface of Titan during the 2004–2014 portion of the *Cassini* mission by the Composite Infrared Spectrometer. Temperatures mapped from pole to pole during five two-year periods show a marked seasonal dependence. The surface temperature near the south pole over this time decreased by 2 K from $91.7 \pm 0.3$ to $89.7 \pm 0.5$ K while at the north pole the temperature increased by 1 K from $90.7 \pm 0.5$ to $91.5 \pm 0.2$ K. The latitude of maximum temperature moved from 19 S to 16 N, tracking the sub-solar latitude. As the latitude changed, the maximum temperature remained constant at $93.65 \pm 0.15$ K. In 2010 our temperatures repeated the north–south symmetry seen by *Voyager* one Titan year earlier in 1980. Early in the mission, temperatures at all latitudes had agreed with GCM predictions, but by 2014 temperatures in the north were lower than modeled by 1 K. The temperature rise in the north may be delayed by cooling of sea surfaces and moist ground brought on by seasonal methane precipitation and evaporation.

*Key words:* infrared: planetary systems – planets and satellites: individual (Titan) – radiation mechanisms: thermal – radiative transfer

## 1. INTRODUCTION

*Cassini* has been observing Titan for more than a third of a Saturnian year. When *Cassini* arrived in 2004 Titan's northern hemisphere was in early winter and in 2014 it was in late spring. During the mission the rate of seasonal change has been great. As the north warms and the south cools, Titan has undergone a reversal in atmospheric circulation that has altered the distribution of gases, clouds, and aerosols on a global scale (West et al. 2011, 2015; Bampasidis et al. 2012; Teanby et al. 2012; Coustenis et al. 2013, 2015; Vinatier et al. 2015). Surface features, particularly at the edges of seas at high southern latitudes, have changed in response to temperature changes (Hayes et al. 2011). Although Titan's lower atmosphere is relatively inert to seasonal temperature variations, sunlight in the visible and near-infrared reaches the surface and the resultant heating drives temperature gradients at the base of the atmosphere. Heat-generated winds near the surface move dune material and drive circulation in the larger seas (Tokano 2008; Rodriguez et al. 2011; Lorenz et al. 2012; Lucas et al. 2014; Tokano & Lorenz 2015a). Evolving global temperatures determine seasonal migrations of surface liquid and vapor distributions and contribute to Titan's methane hydrological cycle (Mitchell et al. 2009; Tan et al. 2015).

We have previously reported the measurement of surface temperatures on Titan by the Composite Infrared Spectrometer (CIRS) on *Cassini* (Flasar et al. 2004; Jennings et al. 2009; Cottini et al. 2012). CIRS detects radiance from the surface at 19 microns wavelength where the atmospheric opacity is a minimum (Samuelson et al. 1981). Data from two time intervals early in the *Cassini* tour, the first during late northern winter (2006–2008) and the second straddling equinox (2008–2010), showed a 0.5 K warming in the north along with a similar cooling in the south (Jennings et al. 2011). Surface temperatures were first measured by *Voyager* in 1980 November (Flasar et al. 1981; Samuelson et al. 1981), so that we now have a baseline of more than a Titan year over which to compare results. In fact, the symmetric north–south temperature distribution that *Voyager* found (Flasar et al. 1981, Courtin & Kim 2002) was repeated at the same epoch (2010) in the CIRS data. In addition to spatial and temporal dependences, Cottini et al. (2012) reported diurnal variations in surface temperature. Janssen et al. (2009, 2015), using *Cassini* 2.18 cm radiometry, found a smaller seasonal variation than CIRS by a factor of 0.87, which they attributed to weaker response at the microwave penetration depth. CIRS has continued to follow Titan's surface temperatures and now has a data set covering 10 years. We report here that over that time the meridional distribution of temperature has progressed from originally having a maximum in the south to presently having a maximum in the north.

## 2. OBSERVATIONS

To examine the time dependence of Titan's surface brightness temperatures, we selected five time periods between 2004 and 2014. Each period spanned approximately two years and provided good latitude coverage by CIRS while being short enough to reveal the seasonal change. The start and end dates for each period were: 2004 October–2006 August, 2006 September–2008 May, 2008 November–2010 May, 2010 December–2012 November, and 2013 April–2014 September. The central solar longitudes for the five periods were $L_s = 313°$, $335°$, $0°$, $28°$, and $53°$. Complete pole-to-pole coverage was achieved for three of the periods, $L_s = 335°$, $0°$ and $53°$, and we included the other two, $L_s = 313°$ and $28°$, for completeness. In the earliest period ($L_s = 313°$) we extended the latitude coverage to the south pole by including one extra

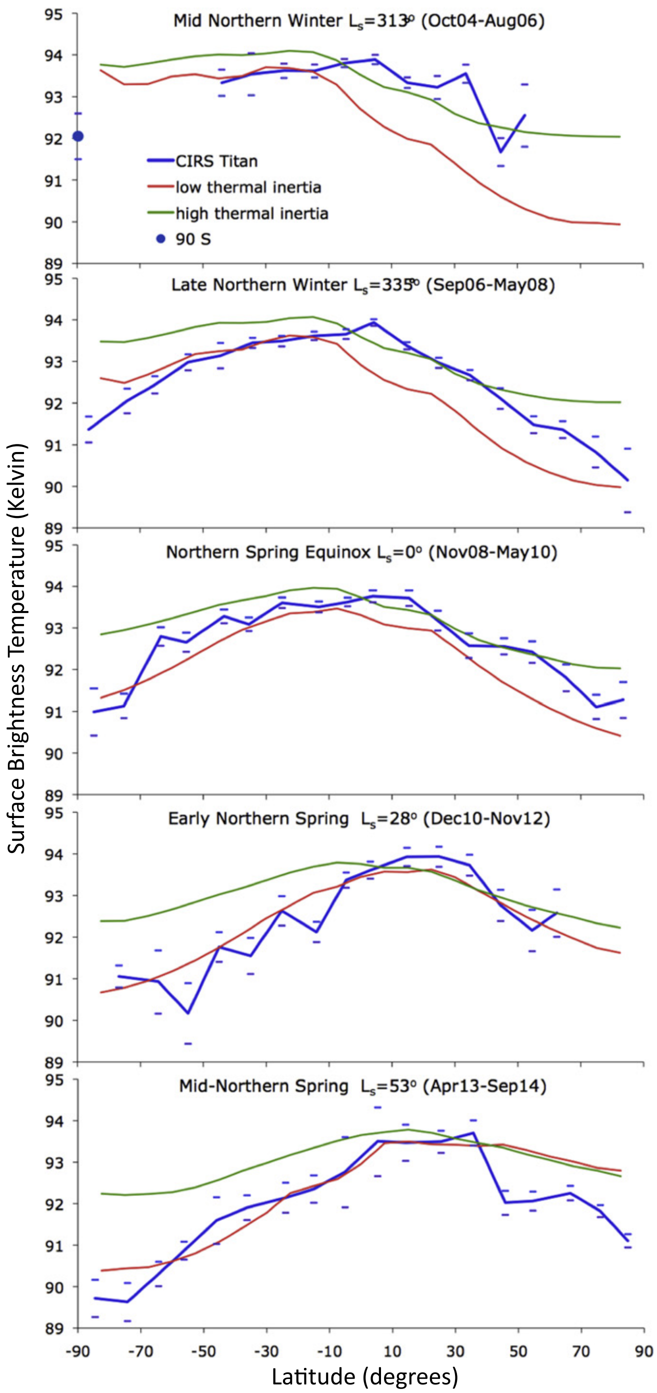


**Figure 1.** Measured surface brightness temperatures (blue) on Titan compared with GCM predictions, for five approximately two-year periods during the *Cassini* mission. The error bars are two standard deviations, calculated from the average that produced each data point. Variation in the size of the error bars is due primarily to differences in the number of spectra averaged. The two GCM curves (Tokano 2005) correspond to low thermal inertia (red) and high thermal inertia (green). Two of the periods, $L_s = 313°$ and 28°, did not have sufficient data to completely map the high latitudes. The single data point at 90 S for $L_s = 313°$, added here to extend the coverage to the south pole, was from 2005 June 6.

observation at 90 S, recorded on 2005 June 6 at a distance of 436,000 km from Titan. For that observation the field of view (FOV) covered 77–90 S.

Spectra within each period were zonally averaged in 10° latitude bins from 90 S to 90 N to create meridional maps. To maintain good sensitivity we only used averages with more than 100 spectra in a bin. The number of spectra in a bin ranged from 117 to 8858 with an average of 1958. To keep the FOV, smaller than about 8° in latitude on the surface, the range from the spacecraft to the target point was limited to less than 140,000 km. The FOV was restricted to be entirely on Titan's disk and emission angles were limited to 0°–50° to avoid the need for large atmospheric corrections. We used spectra from the far-infrared spectral channel of CIRS that covers 10–600 $cm^{-1}$. Most of the spectra were recorded at 15 $cm^{-1}$ resolution, but some were taken from higher resolution data sets and smoothed to 15 $cm^{-1}$. We used a single 15 $cm^{-1}$ resolution element centered at 530 $cm^{-1}$ for measuring the surface radiance. At 530 $cm^{-1}$ the opacity of the atmosphere reaches a minimum in the collisional opacities of $CH_4$–$N_2$ and $H_2$–$N_2$ (Courtin et al. 1995; Samuelson et al. 1997). Molecular emissions below 520 $cm^{-1}$ (Kunde et al. 1981; Coustenis et al. 2008) were avoided. Making our measurements at 530 $cm^{-1}$ permits direct comparison with previous works (Flasar et al. 1981, Jennings et al. 2009, 2011). The CIRS spectra were calibrated using the method described by Flasar et al. (2004).

## 3. DATA ANALYSIS

The surface brightness temperatures were corrected for atmospheric opacity using a model similar to that described by Jennings et al. (2011). The model was adjusted for the central date of each of our five sample periods. The model is based on the temperature profile measured in situ at 0–147 km altitude by the *Huygens* Atmospheric Structure Instrument (HASI) on the *Huygens* descent probe (Fulchignoni et al. 2005). Modifications were applied to the HASI profile to account for latitude dependences and seasonal variations in temperature found by CIRS and *Cassini* radio occultations (Coustenis et al. 2007, 2010, 2013, 2015; Achterberg et al. 2008, 2011; Schinder et al. 2011, 2012; Bampasidis et al. 2012). At latitudes greater than about 60° the stratospheric temperature had a minimum in winter near 120 km. In the model this minimum in the north weakened toward equinox and after equinox began forming in the south. We also included the very low temperatures seen in the atmosphere near the south pole during 2012–2014 (Achterberg et al. 2014; Coustenis et al. 2015; Jennings et al. 2015). The lowest 10 km of the troposphere was transitioned to the surface temperature. Surface relief, local and global, was not treated in the model, but since the temperatures in the lowest 1 km are forced to be close to the surface temperature, the effect of altitude variations is minimal and well within the model approximation. Haze opacity was constant up to 80 km and increased above that with a scale height of 65 km (de Kok et al. 2007; Cottini et al. 2012). The haze opacity increased by 50% from south to north (following Figure 7 in Cottini et al. 2012). The model used a $CH_4$–$N_2$ opacity based on the $CH_4$ altitude profile of Niemann et al. (2010). Absorption coefficients for $CH_4$–$N_2$ were taken from Borysow & Tang (1993) and were increased by 50% following de Kok et al. (2010). We adopted an $H_2$–$N_2$ opacity based on a 0.001 mole fraction of $H_2$ (Courtin et al. 1995; Jennings et al. 2009; Niemann et al. 2010) using $H_2$–$N_2$ absorption coefficients from Courtin (1988) and Dore et al. (1986). Corrections for the atmosphere were all less than 0.2 K, except for the 70–80 S and 80–90 S bins in 2013–2014 ($L_s = 53°$) which, because of the very low atmospheric temperatures at the south pole, required a correction of 0.4 K.

Between 0° and 50° emission angle 80%–70% of the detected radiance originates at Titan's surface. We assumed unit emissivity for Titan's surface at 530 $cm^{-1}$ (Jennings et al. 2011).

## 4. RESULTS AND DISCUSSION

Figure 1 shows our measurements in the five time periods. It is clear that between early and late in the *Cassini* mission the warmest latitudes shifted from south to north of the equator. As they moved northward, the highest temperatures in each period remained about the same. From averages within ±20° of the peak in each period, we found the peak temperatures to be steady at 93.65 ± 0.15 K. At the poles, however, the changes were large. Averages at high latitudes (70°–90°) showed that between 2006 and 2013 ($L_s = 335$–53), temperatures near the north pole increased by 1 K from 90.7 ± 0.5 to 91.5 ± 0.2 K, while temperatures near the south pole decreased by 2 K from 91.7 ± 0.3 to 89.7 ± 0.5 K. We note that in the stratosphere (1–0.1 mbar) between 2010 and 2014 the temperature in the south dropped by about 40 K, whereas in the north it increased by only 6 K (Bampasidis et al. 2012; Coustenis et al. 2015).

Our measurements are compared in Figure 1 with predictions from Tokano (2005). That study used a three-dimensional general circulation model (GCM) of the surface and lower atmosphere to derive surface temperatures as a function of latitude over a Titan year. We take two cases in that study to represent surfaces with low and high thermal inertia: "porous icy regolith" and "rock-ice mixture," respectively, with thermal inertias 335 and 2711 $J\,m^{-2}/\sqrt{s}/K$. Predictions for these two cases are plotted for each of our five time periods. As can be seen from the figure, in the south the temperatures have more closely tracked the low thermal inertia case. In the north, on the other hand, the temperatures have not followed either case. Early in the mission the northern temperatures were aligned with the high thermal inertia case, while most recently ($L_s = 53°$) they have fallen below both cases. The model forecasts 92.7 K near the pole for 2013–2014, but the measured temperature is 91.5 K. The lagging temperatures may be an effect of the seas at northern latitudes. Seas account for 10% the surface area at 55–90 N (Hayes et al. 2011). Le Gall et al. (2015), from 2.18 cm radiometry, report a slower than expected rise in temperature in Ligeia Mare in 2014–2015, possibly revealing the cooling effect of the northern seas. Cooling due to methane evaporation, which may be stronger in the spring as precipitation enhances methane concentrations, will depress sea surface temperatures during early spring (Tokano & Lorenz 2015b). Even without the extra cooling from evaporation, seas have higher thermal inertia than dry land and can be expected to warm more slowly (Tokano 2009). It is not surprising, therefore, that our zonal averages covering both land and seas show temperatures increasing more slowly than land alone.

If the seas are cooled more than the land, however, we would expect to be able to measure a temperature contrast between them. We checked for differences in temperature between land and seas in two ways. First, for the period 2013 April to 2014 September, we looked in the latitude interval 77–83 N both on Legeia Mare (230–260 W) and on land (50–80 W). We found that the land and sea temperatures were the same within the measurement uncertainty, 91.7 ± 0.8 K. Second, for 2012 January to 2015 September, we averaged temperatures over the whole sea district (70–90 N, 230–340 W) and compared this with an average of land temperatures at the same latitudes (50–200 W). Again they were the same within the uncertainty, 91.4 ± 0.3 K. We interpret these measurements to mean that in the north the land is behaving thermally like the sea surfaces and is therefore probably moist (Lora et al. 2015). Evaporation of methane, possibly boosted by spring precipitation, may be cooling the land surface in the same way the sea surfaces are cooled (Tokano & Lorenz 2015b). The temperatures at 46 N and 55 N in our latest period (2013–2014, $L_s = 53°$) appear to be particularly low, possibly also a consequence of cooling at those latitudes. In the south the apparent correspondence of the temperatures to the low thermal inertia case might mean that the land there is drier (Lora & Mitchell 2015). Also, the slower than expected warming in the north may, in part, result from exotic behavior of surface liquids on Titan contemplated by Tan et al. (2015). As the season progresses through late spring and the land dries, temperatures may begin to rise more rapidly.

The conditions for ethane and methane condensation have changed markedly at the poles over the *Cassini* mission (Jennings et al. 2009, 2011). Saturation vapor pressure is strongly dependent on temperature for both species. At the north pole, where temperatures have increased by 1 K, the methane saturation vapor pressure will have increased by 14% and ethane by 25%. At the south pole, where temperatures have decreased by 2 K, the saturation vapor pressure will have decreased by 30% for methane and 40% for ethane. Major changes in condensation are likely to be taking place on the surface at both poles. Both ethane and methane have triple points (90.6 K for methane and 89.9 K for ethane) near the 90 K temperature we most recently measured at 70–90 S.

Huygens HASI measured the surface temperature at 10 S latitude on 2005 January 14 (Fulchignoni et al. 2005). That result, 93.65 ± 0.25 K, agrees within the error with our measurements in 2004–2006 ($L_s = 313°$). Between 2005 and 2013 the temperature at the *Huygens* touchdown latitude had decreased by about 1 K. Our measurements also agree with near-surface temperatures reported by Schinder et al. (2011, 2012) from *Cassini* radio occultations. Their 10 reported ingress and egress surface temperatures, near the same latitudes and dates, were on average 0.25 K lower than CIRS with a standard deviation of 0.45 K.

In previous reports (Jennings et al. 2009; Tan et al. 2015) we presented an analytic formula to describe the latitudinal and seasonal dependence of the surface temperatures. We have updated that formula to include the measurements recorded since those earlier studies. The data in each period were fitted with a cosine latitude profile, which we have found provides a useful match to the shape of the latitude map for each period. The seasonal changes in the temperatures were described by allowing the cosine to vary over time. All measurements from the five periods were fitted at once, with each measurement weighted by its number of spectra. Because the peak temperatures near the equator did not change over the mission we set the amplitude of the cosine to our measured peak value, 93.65 K. The recent depressed temperatures in the north were accounted for by letting the width of the cosine narrow with time. We minimized the standard deviation by adjusting the linear variation of the width and peak latitude. Our result, describing the evolution of surface temperature over 2004–2014 (and not strictly valid outside those years), is given by the formula

$$T = 93.65\cos[(L - (4.2Y - 2.8)) \times (0.000082Y + 0.003)]. \quad (1)$$

Here $L$ is the latitude and $Y$ is the number of years since equinox (2009 August 11). The standard deviation of this formula from the data is 0.4 K. From this formula we see that the peak in the temperature distribution moved from 19 S to 16 N during the mission, roughly tracking the sub-solar latitude. The formula gives the seasonal lag, i.e., the interval following equinox to when the temperature distribution was closest to symmetric about the equator: $\Delta Y \sim 0.7$ yr, or $\Delta L_s \sim 8°$. This is consistent with the lag reported by Janssen et al. (2015) and Jennings et al. (2011). The date corresponding to the seasonal lag was 2010 April, one Titan year after *Voyager 1* found a similar north–south symmetry in surface temperatures (Flasar et al. 1981).

CIRS will add another two-year measurement interval in the remaining portion of the *Cassini* mission leading up to northern summer solstice. By then we anticipate seeing additional changes in the meridional surface temperatures.

The authors acknowledge support from NASA's *Cassini* mission and *Cassini* Data Analysis Program. T. T. was supported by DFG Grant TO269/4-1. We also thank A. Le Gall and M. Janssen for stimulating discussions and for making available preprints of their work.

## REFERENCES

Achterberg, R. K., Conrath, B. J., Gierasch, P. J., Flasar, F. M., & Nixon, C. A. 2008, Icar, 194, 263
Achterberg, R. K., Gierasch, P. J., Conrath, B. J., Flasar, F. M., & Nixon, C. A. 2011, Icar, 211, 686
Achterberg, R. K., Gierasch, P. J., Conrath, B. J., et al. 2014, BAAS, 46, 102.07
Bampasidis, G., Coustenis, A., Achterberg, R. K., et al. 2012, ApJ, 760, 144
Borysow, A., & Tang, C. 1993, Icar, 105, 175
Cottini, V., Nixon, C. A., Jennings, D. E., et al. 2012, P&SS, 60, 62
Courtin, R. 1988, Icar, 75, 245
Courtin, R., Gautier, D., & McKay, C. P. 1995, Icar, 114, 144
Courtin, R., & Kim, S. J. 2002, P&SS, 50, 309
Coustenis, A., Achterberg, R. K., Conrath, B. J., et al. 2007, Icar, 189, 35
Coustenis, A., Bampasidis, G., Achterberg, R. K., et al. 2013, ApJ, 779, 177
Coustenis, A., Jennings, D. E., Achterberg, R. K., et al. 2015, Icar, in press
Coustenis, A., Jennings, D. E., Jolly, A., et al. 2008, Icar, 197, 539
Coustenis, A., Nixon, C. A., Jennings, D. E., et al. 2010, Icar, 207, 461
de Kok, R., Irwin, P. G. J., & Teanby, N. A. 2010, Icar, 209, 854
de Kok, R., Irwin, P. G. J., Teanby, N. A., et al. 2007, Icar, 191, 223
Dore, P., Borysow, A., & Frommhold, L. 1986, JChPh, 84, 5211
Flasar, F. M., Kunde, V. G., Abbas, M. M., et al. 2004, SSRv, 115, 169
Flasar, F. M., Samuelson, R. E., & Conrath, B. J. 1981, Natur, 292, 693
Fulchignoni, M., Ferri, F., Angrilli, F., et al. 2005, Natur, 438, 785
Hayes, A. G., Aharonson, O., Lunine, J. I., et al. 2011, Icar, 211, 655
Janssen, M. A., Le Gall, A., Lopes, R. M., et al. 2015, Icar, in press
Janssen, M. A., Lorenz, R. D., West, R., et al. 2009, Icar, 200, 222
Jennings, D. E., Achterberg, R. K., Cottini, V., et al. 2015, ApJL, 804, L34
Jennings, D. E., Cottini, V., Nixon, C. A., et al. 2011, ApJL, 737, L15
Jennings, D. E., Flasar, F. M., Kunde, V. G., et al. 2009, ApJL, 691, L103
Kunde, V. G., Aikin, A. C., Hanel, R. A., et al. 1981, Natur, 292, 686
Le Gall, A., Malaska, M. J., Lorenz, R. D., et al. 2015, JGRE, submitted
Lora, J. M., Lunine, J. I., & Russell, J. L. 2015, Icar, 250, 516
Lora, J. M., & Mitchell, J. L. 2015, GeoRL, 42, 6213
Lorenz, R. D., Newman, C. E., Tokano, T., et al. 2012, P&SS, 70, 73
Lucas, A., Rodriguez, S., Narteau, C., et al. 2014, GeoRL, 41, 6093
Mitchell, J. L., Pierrehumbert, R. T., Frierson, D. M. W., & Caballero, R. 2009, Icar, 203, 250
Niemann, H. B., Atreya, S. K., Demick, J. E., et al. 2010, JGR, 115, E12006
Rodriguez, S., Le Mouélic, S., Rannou, P., et al. 2011, Icar, 216, 89
Samuelson, R. E., Hanel, R. A., Kunde, V. G., & Maguire, W. C. 1981, Natur, 292, 688
Samuelson, R. E., Nath, N. R., & Borysow, A. 1997, P&SS, 45, 959
Schinder, P. J., Flasar, F. M., Essam, A. M., et al. 2012, Icar, 221, 1020
Schinder, P. J., Flasar, F. M., Marouf, E. A., et al. 2011, Icar, 215, 460
Tan, S. P., Kargel, J. S., Jennings, D. E., et al. 2015, Icar, 250, 64
Teanby, N. A., Irwin, P. G. J., Nixon, C. A., et al. 2012, Natur, 491, 732
Tokano, T. 2005, Icar, 173, 222
Tokano, T. 2008, Icar, 194, 243
Tokano, T. 2009, Icar, 204, 619
Tokano, T., & Lorenz, R. D. 2015a, JGRE, 120, 20
Tokano, T., & Lorenz, R. D. 2015b, Icar, in press
Vinatier, S., Bézard, B., Lebonnois, S., et al. 2015, Icar, 250, 95
West, R. A., Balloch, J., Dumont, P., et al. 2011, GeoRL, 38, L06204
West, R. A., Del Genio, A. D., Barbara, J. M., et al. 2015, Icar, in press